Process for Study of Micro-pilot Diesel-NG Dual Fuel Combustion in a Constant Volume Combustion Vessel Utilizing the Premixed Pre-burn Procedure

Author, co-author (Do NOT enter this information. It will be pulled from participant tab in MyTechZone)

Affiliation (Do NOT enter this information. It will be pulled from participant tab in MyTechZone)

Abstract

A constant volume spray and combustion vessel utilizing the pre-burn mixture procedure to generate pressure, temperature, and composition characteristic of near top dead center (TDC) conditions in compression ignition (CI) engines was modified with post pre-burn gas induction to incorporate premixed methane gas prior to diesel injection to simulate processes in dual fuel engines. Two variants of the methane induction system were developed and studied. The first used a high-flow modified direct injection injector and the second utilized auxiliary ports in the vessel that are used for normal intake and exhaust events. Flow, mixing, and limitations of the induction systems were studied. As a result of this study, the high-flow modified direct injection injector was selected because of its controlled actuation and rapid closure.

Further studies of the induction system post pre-burn were conducted to determine the temperature limit of the methane auto-ignition. It was found that for sufficient induction and mixing time determined from experimental observations and CFD modeling studies, a maximum core temperature of 750 K at the time of micro-pilot diesel injection can be achieved. Although lower than TDC temperatures in diesel CI engines, this temperature is sufficient for studying dual fuel injection and auto-ignition with high cetane fuels. Results from this work confirm the feasibility of dual fuel combustion using the proposed CV process and provide constraints for further micro-pilot diesel-NG dual fuel combustion studies.

Introduction

Natural gas (NG) SI engines are well known, and their application is widespread around the automotive industry. However, current SI engines are limited by compression ratio due to combustion knock. This limitation reduces the potential of utilizing the NG to achieve higher efficiencies and brake mean effective pressure (BMEP) comparable to their diesel counterparts. Therefore, diesel engines that use natural gas as a fuel supplement are a promising alternative due to their higher compression ratio, along with attractive cost and diesel-like performance. Many of the commercially available diesel engines have the capability to be converted to the dual fuel operation principle [1]. There are currently conversion kits available in the market that simply add natural gas injectors into intake ports of conventional diesel engines. In dual fuel natural gas engines, the primary combustion energy comes from burning the natural gas, and a small quantity of diesel liquid fuel is used to initiate the combustion of premixed natural gas and air [2-5].

Conventional pilot-ignited NG combustion has three phases of energy release, including ignition and combustion of the pilot diesel fuel as the diesel pilot spray entrains with the premixed air, combustion of NG in the entrained and in the vicinity of diesel combustion initiated by the pilot fuel energy release, and propagating flame within the NG-air mixture [6]. The diesel pilot fuel amount is typically less than 20% of the total combined NG and diesel fuel energy content [7]. For diesel energy contribution lower than 5%, the diesel injection is referred to as micro-pilot diesel [8, 9].

Several studies are found for conventional diesel pilot-ignited NG engines [6-8, 10-14]. Reduced quantity of diesel pilot has been reported by researchers [15, 16] to improve oxides of nitrogen (NOx) and soot emission commonly seen on normal diesel engines. However, challenges of current dual fuel engines include the high engine-out methane emissions while lean-burn engine operation reduces BMEP and renders the aftertreatment conversion efficiency low. One option to avoid high engine-out methane emissions from excessively lean mixtures, especially at low loads, is to limit (e.g., throttle) the inlet charge flow. This leads to lower in-cylinder temperatures and pressures. These conditions could impact ignition of the diesel pilot, especially for small injection quantities in a micro-pilot application.

Fundamental studies of diesel micro-pilot ignition remain relatively unexplored. In particular, there is a lack of quantitative analysis of diesel ignition for small injection quantities in the presence of premixed natural gas. This work investigates the development of an appropriate test facility and presents quantified ignition results for a micro-pilot dual fuel engine concept.

Diesel and NG studies utilizing the premixed pre-burn process

Optically accessible spray and combustion vessels (S&CV) have been widely utilized for fundamental and detailed investigation into diesel spray and combustion [17-23]. It provides significantly improved optical access compared to other devices, *i.e.*, rapid compression machines and optical engines. Moreover, using a fuel-lean spark-ignited premixed pre-burn process, S&CV can produce a broader range of temperature and pressure in representative of conditions near TDC for most diesel engines [20].

The concept of utilizing fuel-lean spark-ignited premixed burn process to simulate conditions at diesel injection without heating the combustion vessel to high temperatures was initiated by Oren and Ferguson in 1984 [17]. They successfully adopted this methodology in a modified combustion bomb and demonstrated a diesel combustion process at relevant engine conditions. The adoption of the premixed pre-burn process by researchers [18-22] at the Sandia National Laboratories (SNL) and others [24-28] from CMT Motores Temicos and IFP Energies Nouvelles has led to extensive studies for understanding detailed diesel spray and combustion process and have provided valuable insight and knowledge for the advancement of diesel engines, injectors, and impacts of fuels.

Siebers [18] studied the effect of fuel cetane number on ignition delay characteristics in a combustion bomb using the premixed pre-burn process at SNL in 1985. The temperature ranged from 715 K to 1300 K at diesel injection. The premixed pre-burn process was later applied in a high-pressure constant volume combustion vessel developed by SNL. Naber and Siebers [20] explored the effect of gas density on diesel spray characteristics and developed a spray and mixing model covering a wide range of ambient gas densities and temperatures. The model has been shown to accurately predict diesel spray entrainment and penetration by knowing injector geometry, fuel injection momentum, and ambient gas conditions. In a combustion vessel with a high-pressure capability similar to Ref. [20] but in a cubic shaped combustion chamber with better optical accessibility, diesel combustion characteristics were also examined by Pickett *et al.*, including ignition, lift-off length [22, 29], diesel soot emission formation [30], and so forth. A reduced diesel ignition delay was observed in Ref. [22] by increasing ambient temperature, charge density, and fuel cetane number (CN). The maximum ignition delay reported was 2.1 ms for a diesel fuel (CN 46) at an ambient density of 14.8 kg/m^3 and a temperature of 850 K.

Minor species including NO, NO_2, and OH generated during the pre-burn process, and their impact on auto-ignition of diesel surrogates was studies by Nesbitt *et al.* [23]. The experiments with the support of simulations were carried out in a spray and combustion vessel similar to that described in Ref. [22] at Michigan Technological University (MTU). It was found that OH was below 100 ppb and NO, NO_2 were in the 10-30 ppm range during the cool-down process before fuel spray. The effect of these minor species on diesel ignition delay was small, 3% shorter relative to dry air.

The simulated diesel-engine-like conditions based on premixed pre-burn process was also applied to studies of alternative fuel, *i.e.*, NG and methane. The auto-ignition of methane and NG was characterized over a wide range of diesel environment by Fraser *et al*. [31] and Naber *et al*. [32]. The gaseous fuel was directly injected into a combustion vessel the same as Ref. [18] at SNL. The NG ignition delay was above 20 ms at a temperature of 1000 K when NG was injected into an ambient density of 20.3 kg/m^3. Their kinetic model predicted that no ignition occurred at temperatures at and below 950 K.

Summarizing, to develop a premixed NG/air mixture ignited by micro-pilot diesel combustion process in S&CV utilizing pre-mixed pre-burn process followed by NG injection and mixing, the maximum temperature to avoid ignition of NG is 950 K according to the prior work. The micro-pilot diesel operation range relevant to engine conditions has not been identified. The effect of minor species generated by a premixed pre-burn process on diesel combustion is small but is unknown on NG combustion. Although the S&CV with premixed pre-burn process is capable of characterizing micro-pilot diesel spray and combustion without NG over a wide range of dual fuel engine conditions, there is a need to characterize the micro-pilot injection and ignition with NG mixed into the charge gas and to determine the impacts of injection, temperature, pressure, residuals, and fuels on the process.

The objective of the current paper is to develop, demonstrate, and examine a gaseous fuel induction system for dual fuel operation in S&CV using pre-mixed pre-burn procedure and identify system operation limits relevant to engine conditions. The fundamental questions that this research aims to addresses are summarized in Table 1. This initial work uses methane as a surrogate for NG. This will provide the least reactive mixture concerning ignition of the gaseous fuel and thus the minimum constraints.

Table 1. Questions to understand micro-pilot diesel NG dual-fuel combustion process.

Q1	**Can rapid injection and mixing of a gaseous fuel post premixed burn to produce a sufficiently uniform mixture for the subsequent study of diesel pilot injection and dual fuel combustion be achieved?**
Q2	**At what conditions will the methane/post premixed combustion charge mixture auto-ignite post pre-burn as the limit for subsequent micro-pilot diesel injection studies?**
Q3	**How does premixed methane/air composition change before micro-pilot diesel injection?**
Q4	**How well does methane/air mix before injection of micro-pilot diesel fuel?**
Q5	**What is the effect of changing methane/air/dilution parameters on the dual-fuel ignition delay?**

Following from above then, the focus of this work is to determine and demonstrate the capability of the developed process and to provide a clear path for further studies of micro-pilot diesel-NG dual fuel ignition. Presented in this work is the development of dual fuel combustion operation in the S&CV utilizing the premixed pre-burn process. In the Results and Discussion section, flow, mixing and limitations of the methane induction system were studied experimentally and quantitively by CFD analysis. It concludes with a demonstration of a dual fuel combustion process and an ignition investigation of micro-pilot dual fuel combustion process.

Experimental Apparatus

Spray and Combustion Vessel (S&CV)

The Michigan Technological University S&CV is an optically accessible, 1.1 L constant volume combustion vessel [33]. Figure 1 shows the schematic cross-section of the vessel including modifications for the current paper. The 1.1 L cubic-shaped combustion chamber is enclosed by six configurable accessible ports. There are eight auxiliary ports located at corners of the chamber for intake, exhaust and pressure transducer instrumentation.

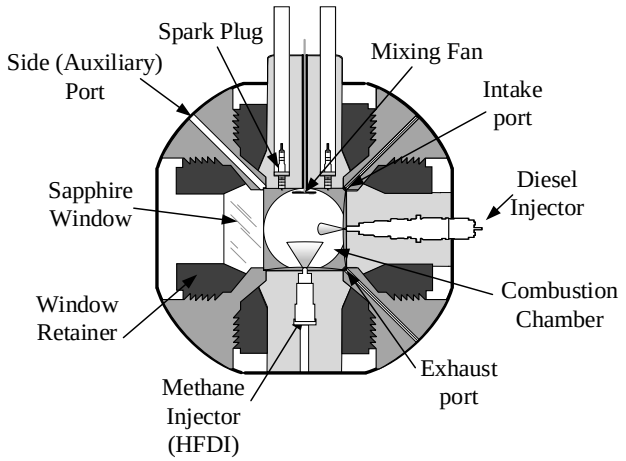

Figure 1. Schematic cross-section of the spray and combustion vessel for dual fuel NG-diesel operation. Note that the sectioned view of auxiliary ports shown in this figure is projected from corresponding corners.

For this research, one accessible port was replaced with a medium-duty diesel injector fixture, as shown in Figure 1. The medium-duty diesel injector used in this study is an 8-hole injector with hole diameters of 0.169 mm and an included angle of 150°. The injector is from a Cummins ISB 6.7L engine that allows a maximum injection pressure up to 2000 bar. A pneumatically driven high-pressure fuel system rated up to 4140 bar was used to feed diesel to the injector [34]. The electrodes that initiate the premixed pre-burn process were mounted in the top port. The top port of the S&CV also had a mixing fan to increase the dilute lean premixed combustion rate and increase the uniformity of the gas temperature post premixed burn. The diesel injector port, the methane injector port, and the top port were installed perpendicularly to each other on the same plane. The remaining accessible ports were installed with sapphire windows to provide nearly complete optical access. Auxiliary ports at the corners of the S&CV were used for gas exchange and pressure transducer instrumentation. A Kistler 6001 pressure transducer was used with a Kistler 5010B charge amplifier to record pressure history at a sample rate of 100 kHz. Also included in Figure 1 are two methane addition systems, the high flow direct injection (HFDI) and side (auxiliary) port, which are discussed in the next sub-section.

Methane Induction System

The methane supply to the gas injection system is achieved by a custom-built methane induction system. The low-pressure methane (<69 bar) is pressurized through a pneumatically driven boost pumping system to a desired upstream pressure (maximum of 350 bar). The high-pressure methane passes through a remotely actuated valve (TESM VAC6PVVA9B9) to control methane supply to a 1-liter accumulator. The volume of the accumulator is designed such that pressure drop due to injection is small ($\Delta P < 2.5$ bar) relative to injection pressure (200 bar), and the flow remains choked under test conditions. The system is also instrumented with a Type K thermocouple and a GT1600 pressure transducer. These provide temperature and pressure measurements before and after the methane injection for mass flow rate estimation. The high-pressure lines are made of one-quarter-inch stainless steel tubes and connected by Swagelok fittings.

The two methane injection methods, HFDI and auxiliary port, were developed and evaluated independently. As shown in Figure 1, an HF DI injector fixture was installed at the bottom port. A modified GDI injector was selected for the rapid methane injection. This DI injector is rated to 300 bar injection pressure. The upper left auxiliary port was modified for methane injection. The design and development of two injection systems are discussed in the later section, and the strategies are examined in the Results and Discussion section. Based on the experimental and the CFD analysis, one of the methane injection systems is to be selected for dual fuel combustion operation utilizing the premixed pre-burn process.

Fuel

Liquid fuel used for the experimental study was VP TORQ performance diesel. In addition, the gaseous fuel was pure methane from the bottle. Properties of the two fuels are provided in Table 2.

Table 2. Properties of diesel and methane fuels used in the experimental study.

Diesel		Density (kg/m^3) @ 15.6 ℃	Heating value (MJ/kg)	Sulfur content (mg/kg)		CN
		784.5	42.8	< 1		85
CH_4	Purity	O_2 (ppm, v/v)	H_2O (ppm, v/v)	N_2 (ppm, v/v)	C_2H_6 (ppm, v/v)	Heating value (MJ/kg)
	99.5%	≤50	≤10	≤4000	≤1000	50

Measurement of the diesel mass flow rate was performed using a Bosch rate of injection (ROI) test rig [35]. The results are taken by averaging accumulated mass of 1000 repeated injections with an injection pressure of 1000 bar and an electrical injection duration (EID) of 0.25 ms. The diesel mass flow rate was held constant at 1.7 mg/stroke for all tests presented in this work. This is equivalent to 1.6% diesel energy contribution for a modified Cummins ISB 6.7L dual fuel engine operating at full load and therefore qualifies as micro-pilot diesel (<5%).

Optical Setup

The optical diagnostic technique used for current work is Schlieren imaging. Using a series of lenses and parabolic mirrors, collimated light is generated through the vessel for Schlieren imaging [34, 36, 37]. The Schlieren technique reveals a density gradient of passing mixture in the chamber and is useful to study dual fuel injection, ignition, and combustion. Images were taken using a Nikon 85 mm camera lens with an aperture size of f/8 on a high-speed camera (FASTCAM SA1.1). The camera was operated at 13,500 and 20,000 frames per second based upon the selection of the field of view. An HPLS-36AD3500 LED base unit coupled with a broadband white light (LEDHR-5500) that has an optical power range of 115-190 mW was used as the light source.

Experimental Procedure

Dual Fuel Process Utilizing Pre-Burn Process

The critical challenge for evaluating dual fuel micro-pilot ignition in the S&CV is to introduce and mix methane after the pre-burn, and before the core area cools below a temperature representative of the compression in a dual fuel engine. The details regarding the standard

pre-burn process can be found in Ref [23]. Figure 2 illustrates an example pressure and temperature history of dual fuel combustion utilizing the premixed pre-burn process. The ambient density, oxygen concentration after pre-burn, core temperature at diesel injection and global equivalence ratio (EQR) were 13 kg/m^3, 16%, 750 K, and 0.54 respectively. The global EQR was based on oxygen content relative to fuel with an H/C ratio of 3.9. The following four steps are conducted in this study:

1. The standard pre-burn process is conducted using a lean mixture of acetylene, hydrogen, oxygen, and nitrogen to generate a high-temperature mixture with the desired oxygen concentration.

2. Post-burn products cool down due to heat transfer.

3a. Inject methane for the period required to obtain the desired global dual fuel EQR before diesel injection.

3b. Wait for a minimum duration (i.e., 50 ms) after methane injection ends to permit mixing of the methane with the post-burn gases.

4. Once diesel trigger condition is reached (e.g., a core temperature of 750 K), diesel injection, diesel auto-ignition, and methane combustion follow.

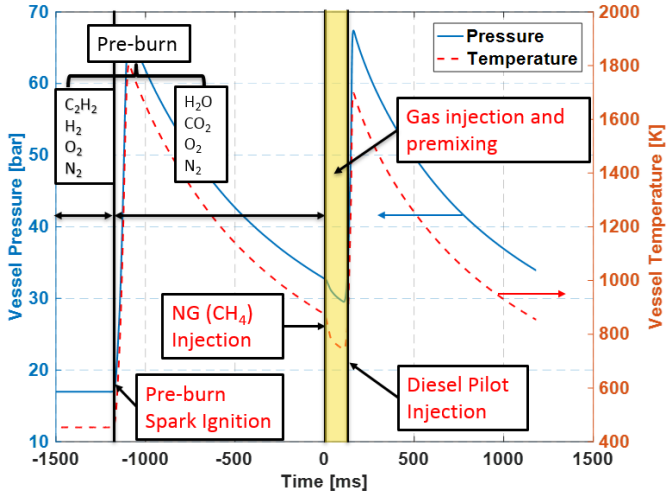

Figure 2. An example in-vessel pressure and temperature history of a dual fuel combustion process. 0 marks the start of methane injection. Experimental conditions were: 13 kg/m^3 ambient density, 16% oxygen concentration after pre-burn before methane injection, 885 K methane injection core temperature, and 750 K diesel injection core temperature. Diesel injection pressure and EID were 1000 bar and 0.25 ms, and 200 bar injection pressure and 33 ms EID for methane injection. The EQR after methane injection was 0.54.

Note that in Figure 2, the temperature was computed using pressure data referred to as the bulk temperature. It is determined from pressure, density, mixture molecular weight, and ideal gas law. The average temperature in the core region is correlated to the vessel wall temperature and the bulk temperature. Detailed discussion on bulk and core temperature can be found in Ref. [20]. An important assumption in developing the correlation is that a stable boundary layer is established. Any events that disrupt the stable boundary layer, *i.e.*, pre-burn combustion, methane injection, render the correlation invalid. Therefore, the temporal temperatures used in Figure 2 and the following figures are bulk temperatures. The boundary layer is well established during cool-down and before methane injection. Once the methane injection is complete, and the momentum of the gas jet decays, and the flow-field is reestablished by the mixing fan. When mixing of the charge gas and methane is complete, the core temperature correlation should once again be valid before diesel injection. This is also evidenced by the vessel pressure decay rate as it returns to its nominal value. Verification of the core to bulk temperature correlation post methane injection via temperature measurements remains to be done. Throughout this paper, the temperature is reported as bulk temperatures unless otherwise specified.

The composition of the charge changes between steps in the process. An example of this is provided in Table 3, which demonstrates how the pre-preburn mixture is composed to achieve a target charge composition. In this case, the target oxygen concentration post preburn was 16%, which represents approximately 32% recirculated exhaust gas (EGR). The addition of methane after the preburn reduces the concentrations of other species and results in a charge mixture that is representative of that found in a premixed charge, dual fuel engine with a relatively high level of EGR.

Table 3. Gas mixture composition at different stages before diesel injection with a desired O_2 concentration of 16% and a methane EQR of 0.58. MF stands for mole fraction.

Conditions		**Composition**						
		C_2H_2	H_2	O_2	N_2	CH_4	H_2O	CO_2
Pre-ignition	MF (%)	3.1	0.5	36.5	59.9	-	-	-
Post pre-burn	MF (%)	-	-	15.9	74.1	-	3.7	6.3
Post CH_4 Inj.	MF (%)	-	-	15.2	70.8	4.6	3.5	6.0

The methane injection system is needed to provide a rapid, controllable, measurable and repeatable methane jet into the combustion chamber during the cool-down process with sufficient momentum to ensure mixing prior to diesel injection. Therefore, the injection needs to be at high velocity to enhance mixing, and short duration to allow more time for mixing. Keeping the flow choked is therefore desired.

The two methane injection systems, developed and evaluated in this work, are shown in Figure 3. One method used a custom nozzle designed to be installed on the auxiliary port shown in Figure 3 (a). The auxiliary port injection system composes of a fast-acting valve (ASCO 8291G410H7100F1), a check valve, a blank auxiliary port, a custom-made nozzle with a center hole diameter of 0.5 mm, high-pressure steel tubes with an inner diameter of 1.6 mm (1/16 of an inch) and a Swagelok fitting. The advantages of an auxiliary port injection system include ease of integration into current S&CV setup and flexible configuration of nozzle geometry. The other method which used the HF DI injector is shown in Figure 3 (b). This includes a modified 5-hole GDI injector with a central hole diameter of 0.5 mm. Although this method poses difficulties of integrating into current S&CV and maximizing mass flow rate, it provides faster actuating time compared with a fast-acting valve used in the auxiliary port methane injection system. Additionally, the relatively large flow passage volume in the auxiliary port injection system leads to continued injection (blow-down) even after the fast-acting valve is

closed until the pressure equalizes. This causes difficulties of controlling methane injection quantity, injection and mixing period, and consequent diesel injection conditions. A quantitative study and comparison are presented in the Results and Discussion section.

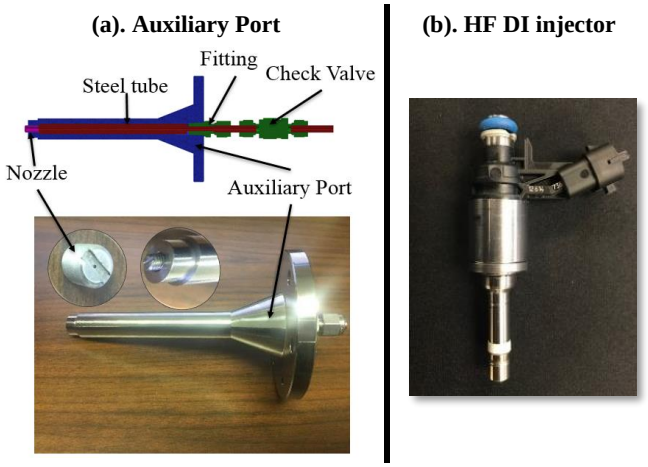

Figure 3. HF DI and auxiliary port systems for methane injection.

Numerical CFD Modelling

A key area of uncertainty in evaluating pilot-ignited premixed combustion in the S&CV is how well mixed the gas is. The vessel is substantially larger than a typical engine, and the flow fields are much less structured, resulting in potentially uneven mixing in the vicinity of the pilot injection. The Schlieren imaging used in the experimental work provides a qualitative, line-of-sight integrated indication of areas of density gradients. To provide a quantified estimate of mixing quality in the vicinity of the pilot injector, a detailed CFD evaluation was undertaken. The CFD evaluation focused on the conditions in the S&CV after the pre-burn event. Both the auxiliary port and the HF DI injection systems were simulated. Dual fuel combustion simulation studies are outside the scope of this paper as the objective is the selection of the gaseous injection system. Therefore, for all the CFD analyses in this paper, there was no micro-pilot diesel injection.

Overview of CFD method

The simulations were carried out using the open source computational fluid dynamics package OpenFOAM which provided the base solver capability of multi-species transport, turbulence modeling and thermo-physical properties and processes such as heat transfer. As this study focused on methane-air mixture preparation post-preburn, most of the modeling conducted was non-reacting. To evaluate the potential for auto-ignition of the methane, a few select cases were conducted including chemical reactions using Westport's dedicated natural gas combustion simulation procedure [38]. This tool uses the conditional source-term estimate to couple the chemical reactions and the turbulent flow field coupling and the trajectory generated lower dimensional manifold (TGLDM) method to perform the detailed chemistry calculations in a tractable time-frame. The chemistry used a previously validated methane reaction mechanism, with 77 species and 379 reactions [39].

The turbulence model employed was the Realizable k-Epsilon model, and the wall temperature of the domain was held constant at 450 K. This was to match the heat transfer rate observed in the experiment. The combustion vessel was equipped with a fan at one of the ports to help with mixing for the pre-burn combustion event. As the axial gas velocity at the downstream side was found to be on the order 5 m/s, the impact of the fan on the mixing for the methane injection was marginal. For comparison, the gas jet velocity is on the order of 200 m/s and would thus be expected to dominate the mixing process. An initial charge motion such that the velocity at the location of the fan of 5 m/s was imposed on the hot gas in the vessel to represent the bulk motion induced by the fan without having to resolve the fan itself.

For simulations involving the high flow injector, which was centrally mounted on one of the vessel ports, the domain was reduced to one-quarter of the combustion vessel with symmetry boundary conditions on each of the planes cutting through the combustion vessel. Though the domain is not strictly symmetric due to the placement of the mounting cone for the diesel injector, the effect was considered to be of secondary importance. The cell size was selected so that the major dimension of the cells near the gas injector would be comparable in size to orifice diameter. Due to the large size of the combustion vessel compared to the orifice diameter, the cell size was expanded geometrically to keep the cell count at approximately 75,000; a sensitivity study of the mesh size near the injector found that this sizing was sufficient to capture the main features of the flow patterns.

The mass injection model was based on the assumption that for the given pressure ratios, the flow through the high flow injector and the auxiliary port orifices would be choked. The total mass of methane required to create a mixture with the target EQR within the vessel domain was calculated, and the mass flow rate through the orifice was calculated and used to set the velocity at the domain inlets. The temperature of the methane fuel entering the domain was 300 K. Methane was allowed to enter the domain via these inlets until the target mass was introduced into the domain.

A three quarter and side view of the high flow domain is shown in Figure 4. Note that the diesel injector location is included for reference only as no dual fuel simulations were carried out for this study.

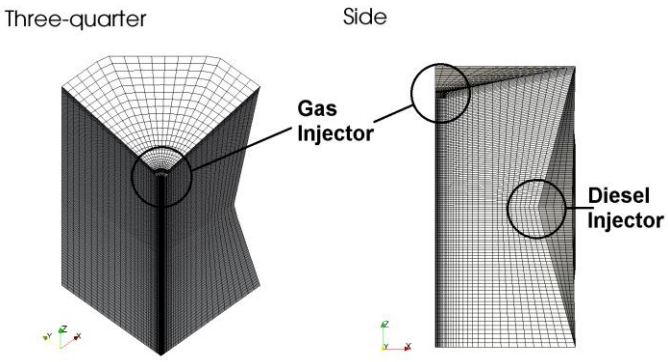

Figure 4. Computational domain for high flow injection simulation

Auxiliary port methane induction domain

Injecting the fuel through the auxiliary port system mounted at the side (auxiliary) port of the combustion vessel required a different symmetry configuration. The domain was split in half by a plane passing through the two opposed auxiliary ports of the combustion vessel, and symmetry boundary conditions were imposed at the split plane once again. Due to the larger size of the domain and slightly

larger orifice size, the cell count was kept to 60000 with similar expansion to the quarter case. Configurations with one and two injection ports were evaluated; the top and side views of this domain are shown in Figure 5.

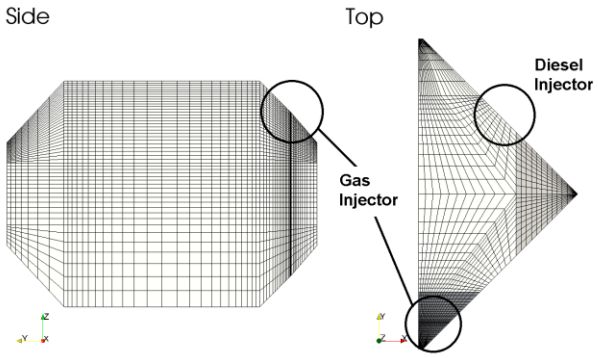

Figure 5. Computational domain for auxiliary port injection simulation

For the auxiliary port configuration, the size of the flow passage volume is such that the blowdown process from this volume constituted an important portion of the injection process; this was simulated by modeling the mass transfer between the accumulator and the combustion vessel with a 0D control volume analysis and calculating the mass flow rate through the injector and gas velocity at the injector exit. For the high flow injector, the internal volume between the injector seat and the orifice is small enough that it had no impact on the mass flow rate at the orifice.

Mixing metrics

One of the key objectives of the study is a quantification of the air-fuel mixing in the combustion vessel near the pilot injector nozzle. Both spatial and temporal variations are important, for two reasons. First, the chamber temperature reduces due to heat transfer during the mixing time – longer mixing times result in lower core temperatures at diesel injection. Second, during gas injection, local conditions could develop that are conducive to auto-ignition of methane. This limits the upper core chamber temperature at which the gas injection can start.

To account for these factors, a mixing quality metric denoted as the mixing index (MI) is used to describe the mixing. The MI for the fuel/air mixture in a specified volume is defined as:

$$MI = \frac{1}{1 + {}^{\sigma}/_{\varphi}} \qquad (1)$$

where σ and φ are the standard deviation and mean of the methane mixture fraction (MMF) respectively. The MMF is a conserved scalar that tracks atoms that originated from the directly-injected fuel., allowing evaluation of mixing independent of combustion.

The MI allows a single number to quantify how uniformly the gaseous fuel has been distributed in the vessel. For direct injection, the MI is initially small with an inhomogeneous mixture. After injection ends and as the mixture becomes more homogeneous, the deviations from the mean are reduced, and the mixing index approaches 1 (in the case of perfect mixing it becomes 1). Prior engine studies at Westport have suggested that an MI of approximately 0.9 or above for premixed engine conditions yielded satisfactory operation; this corresponds to deviations less than 10% of the mean value. The minimum mixing time for CFD studies was defined as the time after the end of injection and the point at which the mixing index reaches a value of at least 0.9.

The mixing index was tracked for both the entire domain as well as a sub-region focused on the pilot ignition zone. Based on characterization studies of the diesel spray penetration, a cylindrical region 50 mm in diameter and 12 mm in height centered on the diesel injector tip was defined for pilot ignition.

Results and Discussion

Flow Characteristics

The methane injection quantity is estimated by ideal gas law using pressure data from the induction system (pressure drop), an in-vessel pressure transducer (pressure rise) under not premixed conditions. Additionally, for cases where combustion occurs, a wideband oxygen sensor is used as a complementary measurement of fuel quantity by measuring the combustion equivalence ratio. The in-vessel pressure history is used here as an example to show the process of estimating methane injection quantity. Methane was injected into the vessel filled with nitrogen to a 27.3 bar pressure and at 453 K. An injection pressure of 69 bar and an EID of 100 ms was used for auxiliary port injection system resulted in a methane quantity of 0.58 g. The same amount of methane quantity was achieved with an injection pressure of 200 bar and an EID of 40 ms for the HF DI injection system.

Figure 6 compares mass injected and mass flow rate of two injection systems. The pressure data was filtered, normalized and then scaled to mass using ideal gas law assuming volume and temperature are constant during injection. A curve was then fitted to the scaled mass data points. The flow rate was obtained by taking its first derivative. The auxiliary port injection system with an injection pressure of 69 bar and an EID of 100 ms (Figure 6a) showed an exponential trend for the methane injection process. After the valve closed, methane trapped in the auxiliary port continued flowing into the vessel until the pressure equalized (blow-down). On the other hand, HF DI system with an injection pressure of 200 bar and an EID of 40 ms (Figure 6b) showed a linear relation between mass and time with only a short opening and closing delay presented (0.2 ms and 0.3 ms respectively). The flow rate of the HF DI system is 14.4 g/s which is significantly higher than the maximum flow rate of 4.7 g/s of the auxiliary port injection system. It was envisioned that the increasing number of auxiliary port nozzles and pressure would increase the total flow rate. However, this would also increase the volume and mass of the methane in the ports. The HF DI system is advantageous because of its rapid closing time and high flow rate.

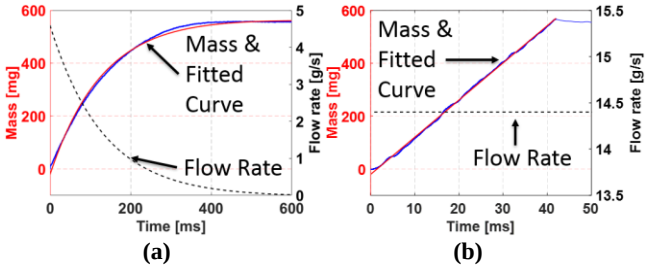

Figure 6. Comparison of mass flow characteristics of auxiliary port (a) and HF DI (b) injection systems. The vessel initially was filled with nitrogen with a

back pressure of 27.3 bar and a temperature of 453 K. For both cases, the resulting methane quantity is 0.58 g.

To determine the injection pressure baseline for the HF DI system, since the flow is choked for all test conditions, increasing mass flow rate can only be achieved by increasing injection pressure and increasing the orifice diameter. At the same injection pressure, increased vessel back pressures as expected do not affect mass flow rate. An injection pressure of 200 bar was selected resulting in a mass flow rate of 14.4 g/s.

CFD Mixing Results

The main focus of the CFD work was on mixing development. This included a comparison of auxiliary port and HF DI strategies and local versus global mixing for the HF DI configuration.

To help guide selection of the fuel induction system, the auxiliary port, and HF DI strategies were compared. Due to the limited amount of computational time available, the conditions evaluated were based on experimental test points and hence are not identical. The cases evaluated are summarized in Table 4. They are representative of a 'best case' for the auxiliary port (low total mass injected), and a representative mid-load case for HF DI strategy. The global mixing index for both cases as a function of the time after the start of injection (ASOI) is shown in Figure 7.

Table 4. Analytical conditions evaluated for mixing study.

Configuration	Injection Pressure	Vessel Pressure	EID	Mixing Time after Injection	Injected Mass
	(bar)	(bar)	(ms)	(ms)	(mg)
HF DI	200	100	120	50	2170
Auxiliary Port	69	17	280	140	550

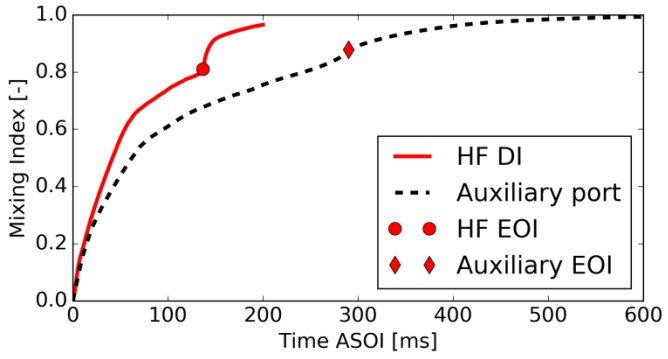

Figure 7. Global mixing index for HF DI and auxiliary port injection systems. Conditions are listed in Table 4.

The time to achieve an acceptable mixing quality is much shorter for the HF DI injection; this is clearly shown in both Figure 7 and Table 4. Despite the lower mass injected with the auxiliary port configuration, the injection duration is substantially longer. This includes both the valve-open period (280 ms vs. 140 ms for the HF DI) and the post-injection 'blow-down'. When the pressure in the system between the fast-acting valve and the auxiliary port nozzle equalizes with the chamber pressure. The HF DI injector also imparts more turbulence, with an average specific turbulent kinetic energy of 3.5 m^2/s^2 compared to 1.5 m^2/s^2 for the auxiliary port configuration.

It was thought that the mixing process for the auxiliary port configuration could be sped up by employing two inlets at opposing ports of the chamber. However, the second injection port has a negative effect on post-injection mixing as the semi-opposed arrangement of the jets results in some of the momentum transfer from the jets being negated. The initial injection time is reduced, but the post-injection mixing time increases.

During injection and mixing, the vessel is losing thermal energy to the surrounding environment and dropping in temperature. In auxiliary port mixing, the introduction of cold fuel into the combustion vessel dropped the core temperature by approximately 50-60 K, comparable to what was seen in the experiment. As the auxiliary port configuration required much longer in the final mixing phase, total heat transfer losses were larger before the minimum mixing time was reached. A simulation of the HF DI injector at a methane injection temperature of 900 K was found to have a temperature at the end of mixing of 750 K. For the auxiliary port with a similar post-injection cooling rate, the temperature would be closer to 650 K, well below the temperature at which diesel would ignite on engine-relevant timescales. As a result, the simulation investigation supports the experimental observations to select the HF DI system for further studies.

Global and Local Mixing Behavior

Thus far the mixing index had been used as a global measure to ensure the uniformity of the gas injection throughout the S&CV. For studies focused on pilot ignition, the critical region is near the pilot injector – the sub-region shown in Figure 4. The global and local average EQR and mixing indices are shown in Figure 8 (a) and Figure 8 (b); the target EQR was 0.57, and the start of injection pressure and temperature were 32 bar and 870 K, respectively.

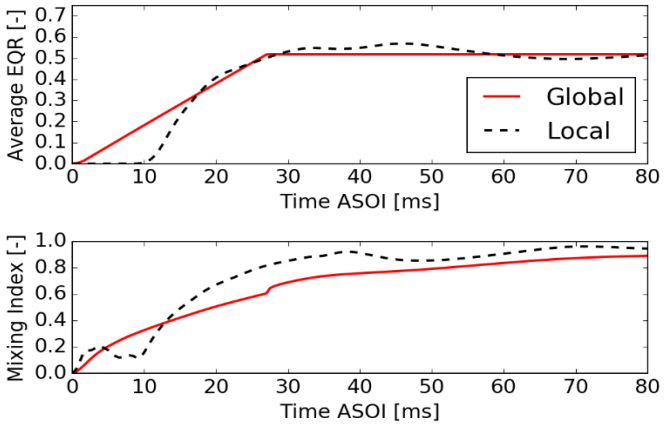

Figure 8. (a) Global and local EQR and (b) mixing indices for methane EQR of 0.57, vessel pressure of 32 bar case with HF DI injection system. Local EQR is for the cylindrical region near the tip of the micro-pilot diesel injector.

As expected, the global average EQR rises linearly to the target and remains there after injection. The local average increases more rapidly as the gas jet impinges on the bottom of the chamber and then recirculates back up into the vicinity of the injector. The MMF can be seen in the time series of S&CV cross sections shown in Figure 9.

While the injection continues, this flow structure remains stable and the local EQR in the near-pilot nozzle region does not change significantly. After injection, the gas jet dissipates rapidly, but residual charge motion reduces the local fuel concentration.

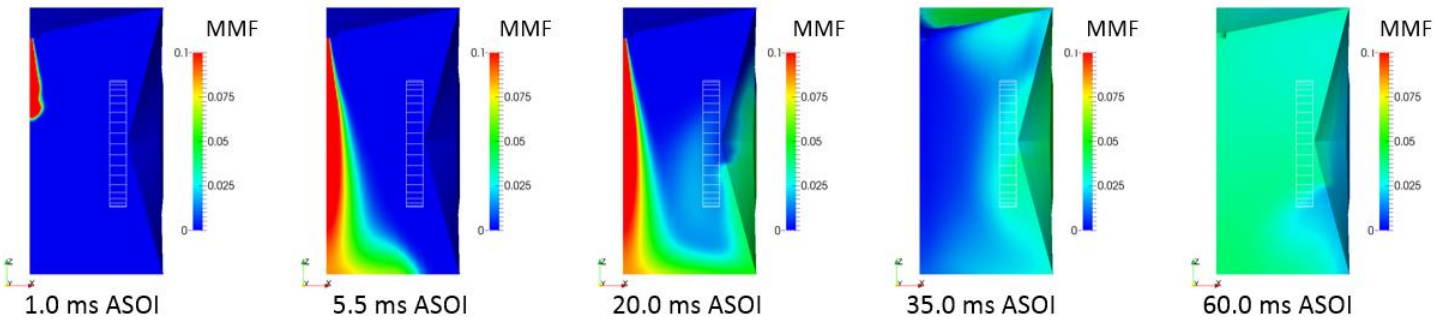

Figure 9. MMF as a function of time. Methane injection pressure, temperature and pressure at methane injection are 200 bar, 870 K, and 36.7 bar, respectively.

Methane Ignition

One of the key limitations of the S&CV with the premixed pre-burn process for premixed methane combustion evaluation is the need to wait until the chamber has cooled sufficiently before starting to inject the methane. Selected reacting-flow cases were conducted to evaluate the likelihood of ignition. In these cases, ignition was identified based on the rapid increase in local temperatures, consumption of CH_4 and appearance of intermediate species (*i.e.*, OH*, CH*, CO).

To provide a consistent definition of ignition time, ignition was defined as a single local temperature exceeding 2000 K. As the exact timing of auto-ignition is not critical for the objective of this work, a more refined definition of ignition is not necessary. However, 2000K was found to correspond well with the appearance of intermediate species and the consumption of methane. An example of one case showing auto-ignition of the methane jet is shown in Figure 10, along with the main diagonal of the combustion vessel. The three contour plots show the MMF, the progress variable distribution of natural gas

combustion (PVD) and the temperature (T). Both progress variable and temperature show a similar distribution, establishing the close correlation of elevated temperature and ignition location in the CFD models.

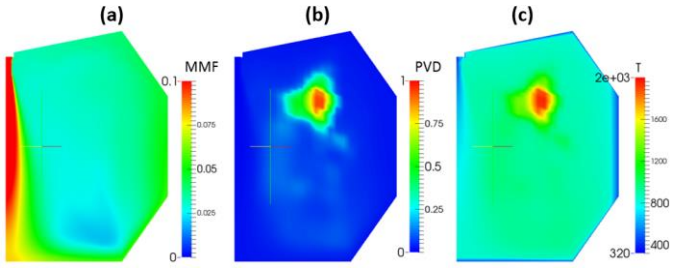

Figure 10. (a) methane mixture fraction (MMF), (b) progress variable distribution (PVD), and (c) vessel temperature (T) for conditions of 134 ms ASOI in the S&CV simulation along main diagonal of the combustion vessel. Methane injection pressure, temperature and pressure at methane injection are 200 bar, 940 K, and 100 bar.

Several cases were run with varying initial temperatures to determine whether the gas would auto-ignite during the injection and mixing stage (*i.e.*, up to 50 ms after the end of injection). The results from these simulations are summarized in Table 5. The results indicated that below an initial (before methane injection) mixture temperature of 900 K, ignition was not observed. This represents an upper limit regarding the operating range of for methane injection. As the temperature in S&CV continues to fall during the post-injection period, it is unlikely that auto-ignition would occur at any point past this.

Table 5. Analytical determination of methane auto-ignition.

Temperature @ Methane Injection K	**Auto-ignition During Mixing Stage**
1000	Yes
940	Yes
< 900	No

An experimental investigation was carried out to explore the upper limit for induction of methane into the post-burn mixture for the creation of conditions for micro-pilot and subsequent dual fuel combustion tests. Table 6 summarizes results for test condition of a constant chamber density of 13 kg/m^3 with 19% O_2 concentration with a methane injection pressure of 200 bar and an EID of 40 ms resulting in methane quantity of 0.58 g and methane EQR of 0.8. For methane injection at 917 K core temperature, all four tests showed that the methane auto-ignited; at 891 K core temperature, two of the three tests auto-ignited. At 885 K core temperature, auto-ignition of the methane did not occur, providing the upper limit for methane induction for the creation of the high pressure premixed methane and 19% air charge for the subsequent micro-pilot diesel injection dual fuel studies. Experimental results are comparable to what were found from the analytical study given in Table 6.

Table 6. Experimental methane auto-ignition limit determination.

Core Temperature @ Methane Injection	**Auto-ignition**	
K	Yes	No
917	4	0
891	2	1
885	0	10
864	0	4

Changes in Gas Composition during Injection

Although the methane injected may not auto-ignite during the mixing time, there remains the possibility that reaction timescales are such that some decomposition of the fuel could occur, and the resultant radicals could impact the diesel ignition delay. To quantify the potential importance of this, a simplified kinetics model using the same combustion chemistry as the CFD model was used to trace the evolution of the species profile for a parcel of fuel injected into the domain. The parcel was modeled as a single volume of premixed fuel/air mixture starting at the oxidizer temperature at the start of injection. The parcel follows the temperature (cooling) profile of the global cooling rate found in the S&CV experiments. As such, this is representative of what the initial portion of the gas jet would experience when it enters the domain and assumes no mixing or other interaction with any other parcel. The previous assumptions would yield the worst case where the mixing of the initial fuel and oxidizer is immediate, while in reality, the mixing process would take a finite amount of time. The target global EQR was set to 0.57, the same value observed in the detailed mixing study.

A sample showing the concentration of OH for the various start of injection temperatures is shown in Figure 11; as can be deduced from the figure, auto-ignition of the parcel occurs at 885 K and 880 K but not at an 875 K starting temperature. The temperature for the non-igniting case (*i.e.*, 875 K) is also shown on the figure.

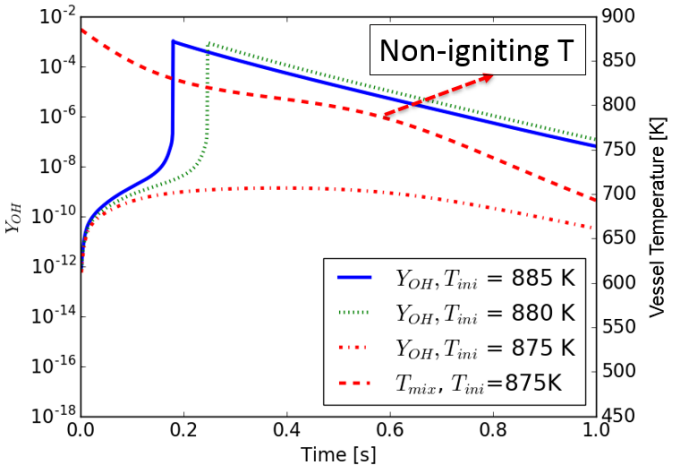

Figure 11. Evolution of OH mass fraction as a function of the start of injection temperature. Methane injection pressure, the pressure at methane injection are 200 bar and 36.7 bar respectively.

For both cases featuring auto-ignition, the mass fraction of OH increases slowly until it reaches 1e-8 after this is it increases rapidly and peaks at 0.001 during ignition and then is consumed. The non-igniting case at 870 K has an OH fraction that levels off at 1e-9, an order of magnitude lower than the OH fraction at the start of ignition and six orders of magnitude below the peak value. The evolution of the mass fraction of methane under the same conditions is shown in Figure 12.

From Figure 12, it is observed that in the non-ignition case, there is still some consumption of methane, roughly 17%. However, this is not representative of the entire mixture, as only the earliest fuel injected will react so quickly. Later fuel will enter a domain that has been cooled both by the incoming gas as well as heat loss to the surroundings. These findings suggest that the final gas composition will be largely unchanged if auto-ignition can be avoided. The temperature threshold of 870 K compares favorably with the experimental findings of 885 K as given in Table 6.

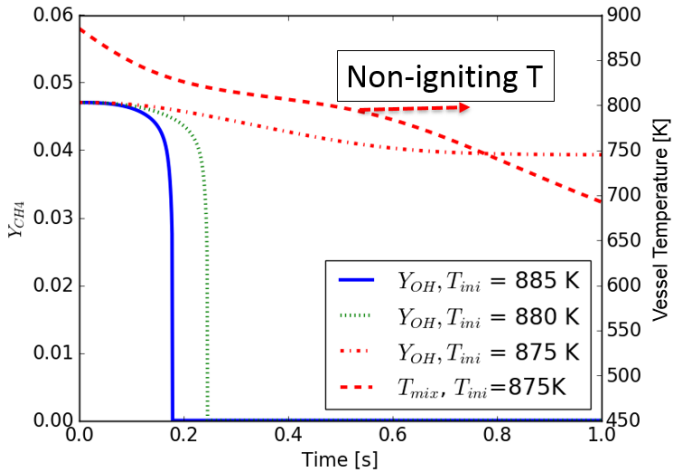

Figure 12. Evolution of methane mass fraction as a function of the start of injection temperature. Methane injection pressure, the pressure at methane injection are 200 bar and 36.7 bar respectively.

Dual Fuel Process Operation Boundaries

The combined effects of methane auto-ignition, methane injection quantity, and mixing time limit the maximum temperature for diesel injection. Figure 13 illustrates an example of pressure and bulk temperature history in determining the diesel injection upper-temperature limit. The changing molecular weight of the mixture due to methane injection is accounted for when computing bulk temperature curve. The upper dash line draws a bulk temperature limit of 870 K for methane auto-ignition. The lower dash line confines upper bulk temperature limit of 742 K for micro-pilot diesel injection given an ambient gas density of 13 kg/m^3, the O_2 concentration of 16%, a methane EQR of 0.74, and a mixing time of 50 ms. A kinetic modeling study was conducted to evaluate the sensitivity of methane auto-ignition to dilution. The effect of dilution on methane auto-ignition was found to be negligible relative to that of oxidizer temperature. Thus, the bulk temperature of 870 K at methane injection was adopted for different oxygen concentrations.

As shown in Figure 13, temperature decreases by 90 K during methane injection period. In addition to heat transfer from the vessel to the surrounding, energy exchange due to injecting low-temperature methane into high-temperature ambient charge plays a crucial role in determining the operating limits for diesel injection. There exists a maximum methane EQR for the desired temperature at diesel injection. However, a richer mixture is achievable with increased dilution. On the one hand, an increased methane EQR due to reduced oxygen concentration results in the same total temperature reduction compared to that of the leaner mixture. Furthermore, the presence of diluent reduces the cooling effect because it effectively provides a higher thermal mass in ambient charge.

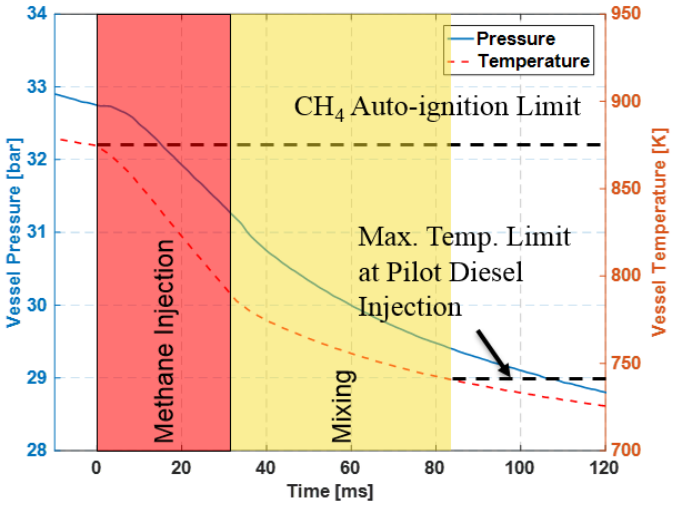

Figure 13. An example of pressure and temperature history of methane injection after pre-burn process demonstrates dual fuel process operation thermal limits. Test conditions were: 16% oxygen concentration, 13 kg/m^3 ambient density and 200 bar methane injection pressure. The methane EQR is 0.74.

Demonstration of A Dual Fuel Combustion Process

The temporal pressure and temperature history obtained from a dual fuel combustion process utilizing the premixed pre-burn process are shown in Figure 14. The vessel was initially filled with a fuel lean pre-burn mixture with a density of 13 kg/m^3. The post-burn gas mixture had an O_2 concentration of 16%. A methane injection pressure of 200 bar and an EID of 25.8 ms resulted in a global EQR of 0.57 measured by a wideband oxygen sensor. Micro-pilot diesel was injected at a core temperature of 750 K with an injection pressure of 1000 bar and a short EID of 0.25 ms. The diesel fuel used was a performance fuel with a cetane number of 85. The corresponding Schlieren images are shown in Figure 15. Another test with same conditions was done to capture Schlieren images focusing on micro-pilot diesel injection, diesel auto-ignition, and consequent methane flame propagation shown in Figure 16.

Shown in Figure 15 is a full view of the combustion chamber at a frame rate of 13500 frames per second. Methane was injected and mixed with the ambient post-burn mixture at time 0, the same as shown in Figure 14. The time of 25.8 ms $ASOI_{Methane}$ marks the end of methane injection ($EOI_{Methane}$). The high-velocity methane jet dissipated quickly. The residual momentum and turbulence from the gas jet continue the methane mixing with the ambient charge until 103 ms $ASOI_{Methane}$ marking the start of diesel injection (SOI_{Diesel}).

Figure 16 focuses in the vicinity of diesel injector at a frame rate of 20000 frames per second. The time of 0 ms in Figure 16 corresponded to the last frame in Figure 15 showing the SOI_{Diesel}. The delay period in this dual fuel combustion consists of coupled processes including: (i) an initial physical delay resulting from diesel fuel atomization and vaporization, (ii) a continued mixing of the diesel fuel with the charged gas, (iii) and a chemical delay occurred simultaneously with the physical delay, which is a result of pre-combustion reactions in the diesel-methane-air-dilution mixture with changing composition based upon the mixing. The auto-ignition of micro-pilot diesel was observed at 2.9 ms $ASOI_{Diesel}$. The ignition was then followed by the methane combustion in the region of the diesel combustion then flame propagation into the remainder of the charge [6].

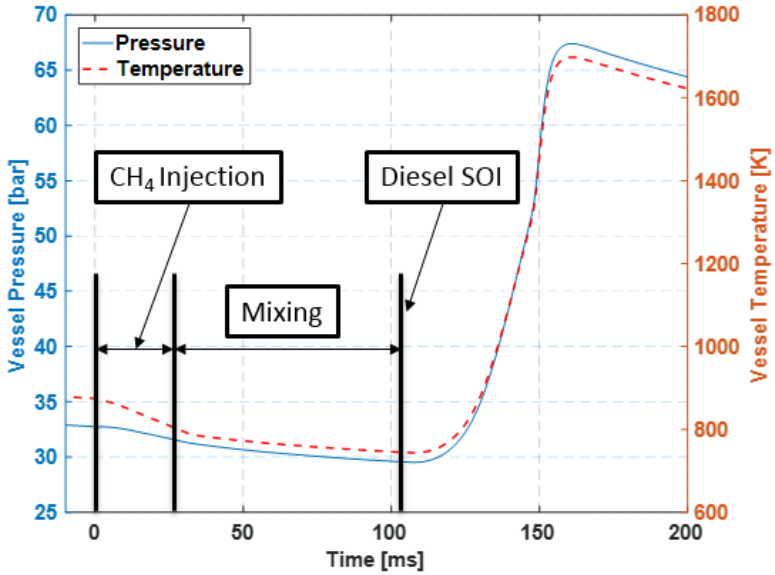

Figure 14. Vessel pressure and temperature traces illustrate a dual fuel combustion process. Test condition: 16% O2, 13 kg/m3, global EQR 0.58, fuel cetane number 85, diesel injection pressure 1000 bar, EID 250 µs, core temperature 749 K at diesel injection. Figure 15 are corresponding Schlieren images showing methane injection and mixing.

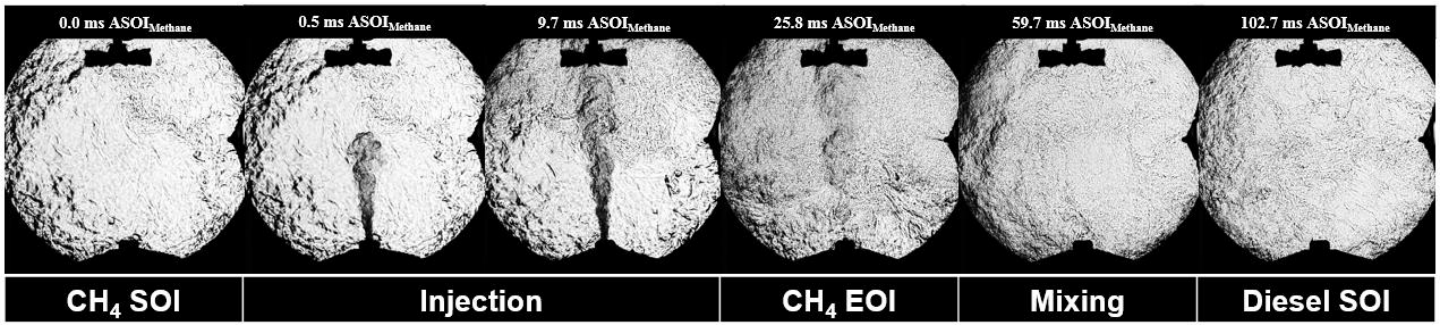

Figure 15. Schlieren images show the methane injection and mixing process. Test conditions are the same as Figure 14: 16% O_2, 13 kg/m^3, global EQR 0.58, and 885 K core temperature at methane injection. Diesel injector is seen on the right side of image; methane injector is at the bottom; the fan is at the top.

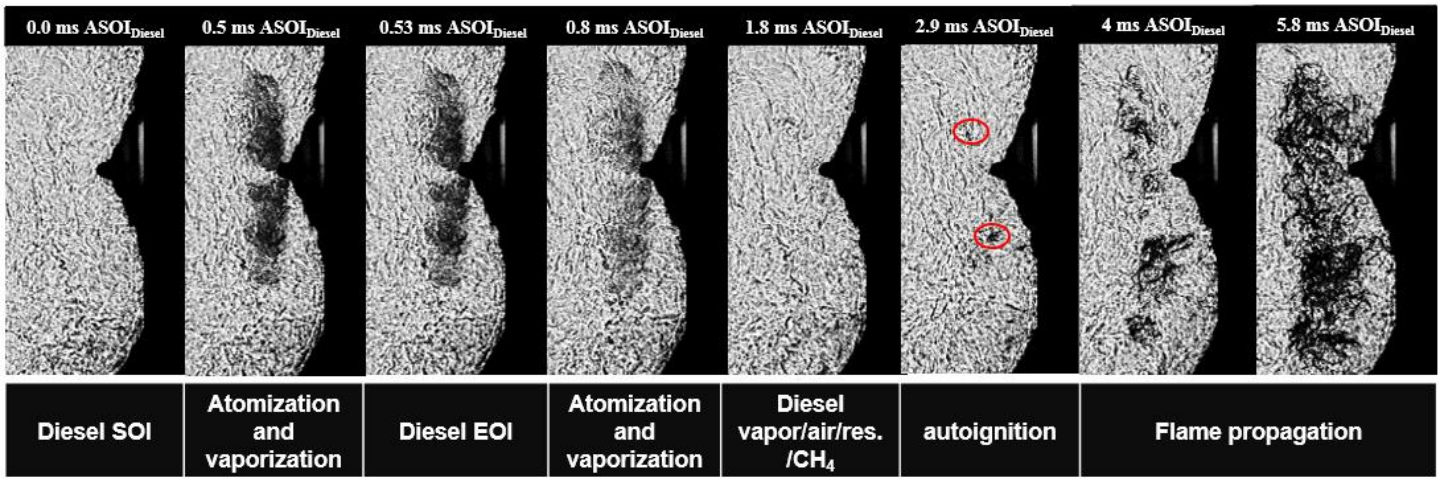

Figure 16. Schlieren images demonstrate diesel injection, auto-ignition, and dual fuel combustion process. Test conditions are the same as Figure 14: 16% O_2, 13 kg/m^3, global EQR 0.58, and 749 K core temperature at diesel injection. The first frame corresponds to the last frame in Figure 15.

To determine the test to test variation, similar test conditions as noted in Figure 14, except for a global EQR of 0.54 were repeated ten times, and the pressure traces are overlaid in Figure 17. Pressure traces were consistent during methane injection period. At the EOI of methane injection, the mean of vessel pressure is 31.3 bar with one standard deviation of 0.1 bar. The variation started at the end of the methane injection event. Since diesel injection was triggered by applying a constant time delay (82 ms in this case) to the SOI of methane injection, the core temperature varied at the time of diesel injection. At diesel injection, the mean value of vessel pressure is 29.7 bar with one standard deviation of 0.2 bar. Converting pressure to core temperature, the mean value of core temperatures is 751 K with one standard deviation of 3 K. The variability of the ignition is further discussed in the next sub-section.

As observed in these tests and through the simulations, it has been shown that using the pre-burn process in an S&CV plus post gaseous injection with sufficient delay for mixing, that conditions representative of in-cylinder conditions for a dual fuel engine can be repeatably created within the limits of methane autoignition. Subsequent micro-pilot diesel injection into this charge gas with methane is shown to ignite repeatably with ignition delays representative of dual fuel combustion engines.

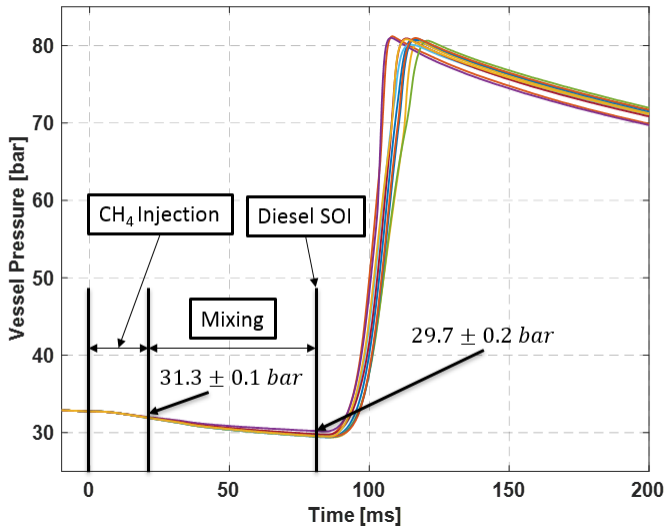

Figure 17. Overlay of 10 repeated dual fuel combustion tests. Test conditions are 16% O_2, 13 kg/m^3, 0.54 global EQR, 85 CN. Diesel injection pressure, EID, the core temperature at methane injection and desired core temperature at diesel injection were 1000 bar, 250 µs, 885 K and 750 K.

Effect of Premixed Methane on Dual Fuel Ignition Delay

To demonstrate the application of the S&CV study for dual fuel engine conditions, a single condition was selected for testing with and without premixed methane. Figure 18 compares the ignition delays of diesel fuel only to that of diesel-NG dual fuel combustion. Results of dual fuel ignition delay were obtained from tests shown in Figure 17. Injecting the single diesel fuel was achieved by disabling methane injector and injecting diesel at the same density and core temperature as those for dual fuel tests.

Given that a very small quantity of diesel fuel was used, the pressure rise caused by ignition is small compared to the ambient pressure when diesel was injected. Thus, there is a lack of measurable initiation of combustion from the pressure signal for determination of the ignition delay. The ignition delay in this work is defined as the time between the start of diesel injector hydraulic opening and the first frame that diesel auto-ignition is identified in Schlieren images. For both cases, ignition delays are the mean values of 10 repeated tests with error bars indicating one standard deviation. The coefficient of variation (COV), a division of one standard deviation over the mean, is 0.1 for both cases indicating that repeatable ignition is achievable from test to test.

It is observed that, with the presence of premixed methane in the post-burn mixture, the diesel auto-ignition is significantly postponed approximately two times than that for single diesel fuel case. The prolonged ignition delay period was comparable to calculated results using fully detailed kinetics for n-heptane and methane mixture under constant volume adiabatic conditions [40]. The experimental results from this work are also consistent with the findings in Ref. [40] that at least 55 percent methane by volume (95 percent locally for this work) of n-heptane and methane mixture is required to produce an ignition delay as twice as that for pure n-heptane. According to the kinetic study, the difference of ignition delay could be explained by changes of reaction rate and concentration of key transient products with the presence of premixed methane/air mixture.

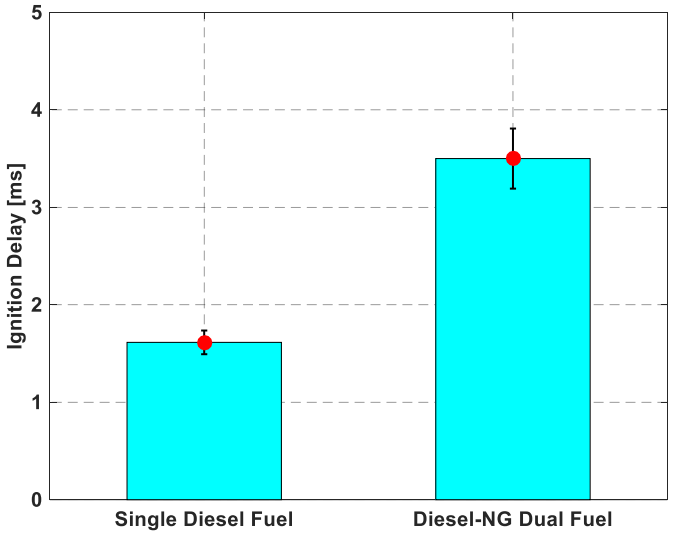

Figure 18. Comparison of ignition delay for single diesel fuel to diesel-NG dual fuel. Dual fuel test conditions were the same as in Figure 17. Single diesel fuel was conducted at the same density of 13 kg/m^{3,} and a core temperature of 750 K at diesel injection. Diesel fuel cetane number was 85 for both cases.

Summary and Conclusions

A diesel micro-pilot methane dual fuel combustion process was developed utilizing the two-stage premixed pre-burn plus post gaseous methane injection process. Hardware and process development with integrated CFD studies of the methane mixing and ignition were presented. To the best of authors' knowledge, this work is the ***first study*** undertaken to apply the two-stage pre-burn and post gas injection method in a constant volume combustion vessel to create engine thermodynamic and premixed conditions representative of a dual fuel engine. Details of the mixing of the methane post gas injection are examined and quantified utilizing CFD. Further micro-pilot ignition of a premixed methane + air + dilution homogeneous mixture was shown to be controllable and repeatable with respect to conditions at the start of the diesel pilot injection.

Table 7. Summary of technical approaches developed to answer the questions in Table 1.

Q1	**S&CV pressure trace and Schlieren images**
Q2	**S&CV pressure trace and Schlieren images, and CFD**
Q3	**Non-reacting CFD simulations**
Q4	**S&CV Schlieren images and CFD**
Q5	**S&CV Schlieren images**

Approaches that are used to address the questions listed in Table 1 are summarized in Table 7. Findings and observations from the experimental and analytical CFD studies include:

1. The maximum temperature at the time of diesel injection that can be achieved is a function of (i) the maximum temperature for methane auto-ignition; (ii) the mass of methane injected relative to total charge mass; (iii) and the time required to mix the methane and post-burn gas to an acceptable MI of 0.8.

2. The CFD study of the resulting methane mixing post injection near the diesel injector tip was found to reach an acceptable level of homogeneity (mixing index > 0.8) after 50 ms post end of gaseous injection for most conditions. This was 20 ms shorter than that found in global mixing quality.

3. Reacting flow simulations determined that the injected methane would likely auto-ignite for chamber temperatures above 900 K; these agreed with experimental measurements. This temperature establishes an upper limit on both methane gas and subsequent diesel injection for dual fuel combustion studies.

4. Chemical kinetic models were used to trace the evolution of species mass fractions in a portion of mixing fuel and air to determine if final mixtures profiles would suffer significant changes. It was found that if methane auto-ignition could be avoided there would be negligible changes in gas composition to impact the diesel pilot ignition process.

5. Repeated tests showed that the combustion vessel ambient pressure is repeatable, resulting in only 3 K difference of the

core temperature in the estimated temperature at the time of diesel injection.

6. Auto-ignition of diesel micro-pilot is significantly retarded in the presence of methane in the premixed gases due to changes in reaction rate and concentration of transient products. Results such as these will be critical to further study the dual fuel ignition process in diesel-NG fueled engines.

For future work, considering limitations of the current dual fuel combustion process in S&CV, ignition characterization and modeling of micro-pilot diesel are of great interest to ensure a sustainable ignition and combustion strategy. Results from these studies will support CFD model validation under engine representative conditions and provide the data needed to develop reduced order ignition delay models for utilization in 1D engine simulation and other tools.

References

1 Wei, L. and Geng, P., "A Review on Natural Gas/Diesel Dual Fuel Combustion, Emissions and Performance," *Fuel Processing Technology* 142(264-278, 2016, doi:https://doi.org/10.1016/j.fuproc.2015.09.018.

2 Manns, H.J., Brauer, M., Dyja, H., Beier, H., and Lasch, A., "Diesel Cng - the Potential of a Dual Fuel Combustion Concept for Lower Co2 and Emissions," SAE Technical Paper 2015-26-0048, 2015, doi:https://doi.org/10.4271/2015-26-0048.

3 Karim, G.A., "A Review of Combustion Processes in the Dual Fuel Engine—the Gas Diesel Engine," *Progress in Energy and Combustion Science* 6(3):277-285, 1980, doi:https://doi.org/10.1016/0360-1285(80)90019-2.

4 Karim, G.A. and Ali, I.A., "Combustion, Knock and Emission Characteristics of a Natural Gas Fuelled Spark Ignition Engine with Particular Reference to Low Intake Temperature Conditions," *Proceedings of the Institution of Mechanical Engineers* 189(1):139-147, 1975, doi:10.1243/PIME_PROC_1975_189_020_02.

5 Cho, H.M. and He, B.-Q., "Spark Ignition Natural Gas Engines—a Review," *Energy Conversion and Management* 48(2):608-618, 2007, doi:https://doi.org/10.1016/j.enconman.2006.05.023.

6 Karim, G.A., "Combustion in Gas Fueled Compression: Ignition Engines of the Dual Fuel Type," *Journal of Engineering for Gas Turbines and Power* 125(3):827-836, 2003, doi:10.1115/1.1581894.

7 Singh, S., Kong, S.-C., Reitz, R.D., Krishnan, S.R., and Midkiff, K.C., "Modeling and Experiments of Dual-Fuel Engine Combustion and Emissions," SAE Technical Paper 2004-01-0092, 2004, doi:https://doi.org/10.4271/2004-01-0092.

8 Weaver, C.S. and Turner, S.H., "Dual Fuel Natural Gas/Diesel Engines: Technology, Performance, and Emissions," SAE Technical Paper 940548, 1994, doi:https://doi.org/10.4271/940548.

9 Eichmeier, J., Wagner, U., and Spicher, U., "Controlling Gasoline Low Temperature Combustion by Diesel Micro Pilot Injection," *Journal of Engineering for Gas Turbines and Power* 134(7):072802-072802-072809, 2012, doi:10.1115/1.4005997.

10 Papagiannakis, R.G., Hountalas, D.T., Rakopoulos, C.D., and Rakopoulos, D.C., "Combustion and Performance Characteristics of a Di Diesel Engine Operating from Low to High Natural Gas Supplement Ratios at Various Operating Conditions," SAE Technical Paper 2008-01-1392, 2008, doi:https://doi.org/10.4271/2008-01-1392.

11 Kusaka, J., Okamoto, T., Daisho, Y., Kihara, R., and Saito, T., "Combustion and Exhaust Gas Emission Characteristics of a Diesel Engine Dual- Fueled with Natural Gas," *JSAE Review* 21(4):489-496, 2000, doi:https://doi.org/10.1016/S0389-4304(00)00071-0.

12 Gebert, K., Beck, N.J., Barkhimer, R.L., Wong, H.-C., and Wells, A.D., "Development of Pilot Fuel Injection System for Cng Engine," SAE Technical Paper 961100, 1996, doi:https://doi.org/10.4271/961100.

13 Khosravi, M., Rochussen, J., Yeo, J., Kirchen, P., McTaggart-Cowan, G., and Wu, N., "Effect of Fuelling Control Parameters on Combustion Characteristics of Diesel-Ignited Natural Gas Dual-Fuel Combustion in an Optical Engine," presented at ASME 2016 Internal Combustion Engine Division Fall Technical Conference, 2016.

14 Liu, J., Yang, F., Wang, H., Ouyang, M., and Hao, S., "Effects of Pilot Fuel Quantity on the Emissions Characteristics of a Cng/Diesel Dual Fuel Engine with Optimized Pilot Injection Timing," *Applied Energy* 110(201-206, 2013, doi:https://doi.org/10.1016/j.apenergy.2013.03.024.

15 Papagiannakis, R.G. and Hountalas, D.T., "Experimental Investigation Concerning the Effect of Natural Gas Percentage on Performance and Emissions of a Di Dual Fuel Diesel Engine," *Applied Thermal Engineering* 23(3):353-365, 2003, doi:https://doi.org/10.1016/S1359-4311(02)00187-4.

16 Lounici, M.S., Loubar, K., Tarabet, L., Balistrou, M., Niculescu, D.-C., and Tazerout, M., "Towards Improvement of Natural Gas-Diesel Dual Fuel Mode: An Experimental Investigation on Performance and Exhaust Emissions," *Energy* 64(200-211, 2014, doi:https://doi.org/10.1016/j.energy.2013.10.091.

17 Oren, D.C., Wahiduzzaman, S., and Ferguson, C.R., "A Diesel Combustion Bomb: Proof of Concept," SAE Technical Paper 841358, 1984, doi:https://doi.org/10.4271/841358.

18 Siebers, D.L., "Ignition Delay Characteristics of Alternative Diesel Fuels: Implications on Cetane Number," SAE Technical Paper 852102, 1985, doi:https://doi.org/10.4271/852102.

19 Siebers, D.L. and Edwards, C.F., "Autoignition of Methanol and Ethanol Sprays under Diesel Engine Conditions," SAE Technical Paper 870588, 1987, doi:https://doi.org/10.4271/870588.

20 Naber, J. and L. Siebers, D., "Effects of Gas Density and Vaporization on Penetration and Dispersion of Diesel Sprays," 105(82-111, 1996, doi:10.4271/960034.

21 Siebers, D.L., "Liquid-Phase Fuel Penetration in Diesel Sprays," SAE Technical Paper 1998, doi:https://doi.org/10.4271/980809.

22 Pickett, L.M., Siebers, D.L., and Idicheria, C.A., "Relationship between Ignition Processes and the Lift-Off Length of Diesel Fuel Jets," SAE Technical Paper 2005-01-3843, 2005, doi:https://doi.org/10.4271/2005-01-3843.

23 Nesbitt, J.E., Johnson, S.E., Pickett, L.M., Siebers, D.L., Lee, S.-Y., and Naber, J.D., "Minor Species Production from Lean Premixed Combustion and Their Impact on Autoignition of Diesel Surrogates," *Energy & Fuels* 25(3):926-936, 2011, doi:10.1021/ef101411f.

24 Payri, F., Pastor, J.V., Nerva, J.-G., and Garcia-Oliver, J.M., "Lift-Off Length and Kl Extinction Measurements of Biodiesel and Fischer-Tropsch Fuels under Quasi-Steady Diesel Engine Conditions," *SAE International Journal of Engines* 4(2):2278-2297, 2011, doi:https://doi.org/10.4271/2011-24-0037.

25 Skeen, S.A., Manin, J., Pickett, L.M., Cenker, E., Bruneaux, G., Kondo, K., Aizawa, T., Westlye, F., et al., "A Progress Review on Soot Experiments and Modeling in the Engine Combustion Network (Ecn)," *SAE International Journal of Engines* 9(2):883-898, 2016, doi:https://doi.org/10.4271/2016-01-0734.

26 Pastor, J., Garcia-Oliver, J.M., Garcia, A., Zhong, W., Micó, C., and Xuan, T., "An Experimental Study on Diesel Spray Injection into a Non-Quiescent Chamber," *SAE International Journal of Fuels and Lubricants* 10(2):394-406, 2017, doi:https://doi.org/10.4271/2017-01-0850.
27 Malbec, L.-M. and Bruneaux, G., "Study of Air Entrainment of Multi-Hole Diesel Injection by Particle Image Velocimetry - Effect of Neighboring Jets Interaction and Transient Behavior after End of Injection," *SAE International Journal of Engines* 3(1):107-123, 2010, doi:https://doi.org/10.4271/2010-01-0342.
28 Eagle, W.E., Malbec, L.-M., and Musculus, M.P., "Measurements of Liquid Length, Vapor Penetration, Ignition Delay, and Flame Lift-Off Length for the Engine Combustion Network 'Spray B' in a 2.34 L Heavy-Duty Optical Diesel Engine," *SAE International Journal of Engines* 9(2):910-931, 2016, doi:https://doi.org/10.4271/2016-01-0743.
29 Pickett, L.M., Kook, S., and Williams, T.C., "Transient Liquid Penetration of Early-Injection Diesel Sprays," *SAE International Journal of Engines* 2(1):785-804, 2009, doi:https://doi.org/10.4271/2009-01-0839.
30 Pickett, L.M. and Siebers, D.L., "An Investigation of Diesel Soot Formation Processes Using Micro-Orifices," *Proceedings of the Combustion Institute* 29(1):655-662, 2002, doi:https://doi.org/10.1016/S1540-7489(02)80084-0.
31 Fraser, R.A., Siebers, D.L., and Edwards, C.F., "Autoignition of Methane and Natural Gas in a Simulated Diesel Environment," SAE Technical Paper 910227, 1991, doi:https://doi.org/10.4271/910227.
32 Naber, J.D., Siebers, D.L., Caton, J.A., Westbrook, C.K., and Di Julio, S.S., "Natural Gas Autoignition under Diesel Conditions: Experiments and Chemical Kinetic Modeling," SAE Technical Paper 942034, 1994, doi:https://doi.org/10.4271/942034.
33 Zhao, L., Torelli, R., Zhu, X., Naber, J., Lee, S.-Y., Som, S., Scarcelli, R., and Raessi, M., "Evaluation of Diesel Spray-Wall Interaction and Morphology around Impingement Location," SAE Technical Paper 2018-01-0276, 2018, doi:https://doi.org/10.4271/2018-01-0276.
34 Tang, M., Zhao, L., Lee, S.-Y., and Naber, J., "Effect of Combustion on Diesel Spray Penetrations in Relation to Vaporizing, Non-Reacting Sprays," SAE Technical Paper 2016-01-2201, 2016, doi:https://doi.org/10.4271/2016-01-2201.
35 Bower, G.R. and Foster, D.E., "A Comparison of the Bosch and Zuech Rate of Injection Meters," SAE Technical Paper 910724, 1991, doi:https://doi.org/10.4271/910724.
36 Parrish, S.E., "Evaluation of Liquid and Vapor Penetration of Sprays from a Multi-Hole Gasoline Fuel Injector Operating under Engine-Like Conditions," *SAE International Journal of Engines* 7(2):1017-1033, 2014, doi:https://doi.org/10.4271/2014-01-1409.
37 Zhang, A., Montanaro, A., Allocca, L., Naber, J., and Lee, S.-Y., "Measurement of Diesel Spray Formation and Combustion Upon Different Nozzle Geometry Using Hybrid Imaging Technique," *SAE International Journal of Engines* 7(2):1034-1043, 2014, doi:https://doi.org/10.4271/2014-01-1410.
38 McTaggart-Cowan, G., Mann, K., Huang, J., Singh, A., Patychuk, B., Zheng, Z.X., and Munshi, S., "Direct Injection of Natural Gas at up to 600 Bar in a Pilot-Ignited Heavy-Duty Engine," *SAE International Journal of Engines* 8(3):981-996, 2015, doi:https://doi.org/10.4271/2015-01-0865.
39 Huang, J., Hill, P.G., Bushe, W.K., and Munshi, S.R., "Shock-Tube Study of Methane Ignition under Engine-Relevant Conditions: Experiments and Modeling," *Combustion and Flame* 136(1):25-42, 2004, doi:https://doi.org/10.1016/j.combustflame.2003.09.002.
40 Khalil, E. and Karim, G., "A Kinetic Investigation of the Role of Changes in the Composition of Natural Gas in Engine Applications," *Journal of engineering for gas turbines and power* 124(2):404-411, 2002, doi:http://dx.doi.org/10.1115/1.1445438.

Contact Information

Xuebin Yang
Michigan Technological University
Email: xuebiny@mtu.edu

Professor Jeffrey D. Naber
Michigan Technological University
Email: jnaber@mtu.edu

Acknowledgments

Financial support for this research was provided by DOE under contract No. EE0007331 and by Westport Fuel Systems Inc. The experimental work was performed at the Alternative Energy Research Building, Advanced Power Systems Laboratories with the assistance and advice of co-workers: H. Schmidt and W. Atkinson. We would also like to thank Westport Fuel Systems research team for the technical contribution and discussions provided in the development of the process presented in this work.

Definitions/Abbreviations

TDC	Top dead center
CFD	Computational fluid dynamics
CI	Compression ignition
SI	Spark ignition
BMEP	Break mean effective pressure
NG	Natural Gas
NOx	Oxides of nitrogen
S&CV	Spray & Combustion Vessel
SNL	Sandia National Laboratories
CN	Cetane number
MTU	Michigan Technological University
HF DI	High flow direct injection
GDI	Gasoline direct injection
EQR	Equivalence ratio

MF	Mole fraction
EID	Electronic injection duration
EGR	Exhaust gas recirculation
TGLDM	Trajectory generated lower dimensional manifold
MI	Mixing index
MMF	Methane mixture fraction
PVD	Progress variable distribution
$ASOI_{Methane}$	After the start of methane injection
$EOI_{Methane}$	End of methane injection
$ASOI_{Diesel}$	After the start of diesel injection
COV	Coefficient of variation